Macromolecules

Cite This: Macromolecules 2018, 51, 7713−7721

Article

pubs.acs.org/Macromolecules

Stability of Two-Dimensional Dodecagonal Quasicrystalline Phase of Block Copolymers

Chao Duan,[†,‡] Mingtian Zhao,[†,‡] Yicheng Qiang,[†,‡] Lei Chen,[†] Weihua Li,[*,†] Feng Qiu,[†] and An-Chang Shi[§]

[†]State Key Laboratory of Molecular Engineering of Polymers, Key Laboratory of Computational Physical Sciences, Department of Macromolecular Science, Fudan University, Shanghai 200433, China

[§]Department of Physics and Astronomy, McMaster University, Hamilton, Ontario L8S 4M1, Canada

Supporting Information

ABSTRACT: Quasicrystalline (QC) phases have been observed in various condensed matter systems including self-assembling block copolymer (BCP) melts. Theoretical study of the thermodynamic stability of QC phases presents a long-standing unsolved problem because of the aperiodic nature of the structures. Here, we report a combination method to study the thermodynamic stability of two-dimensional dodecagonal quasicrystalline (DDQC) phase with both ideal tiling and random tiling patterns formed by ABCB tetrablock terpolymers. This method applies the self-consistent field theory coupled with the Stampfli self-similarity construction to accurately calculate the free energy of the periodic DDQC approximants and then uses a cluster model to predict the stability of aperiodic DDQC phase. Surprisingly, we find a stable DDQC approximant but metastable ideal tiling DDQC structures. Moreover, the random tiling DDQC structures as a mesoscopic coexistence of two neighboring periodic substructures of DDQC might become stable.

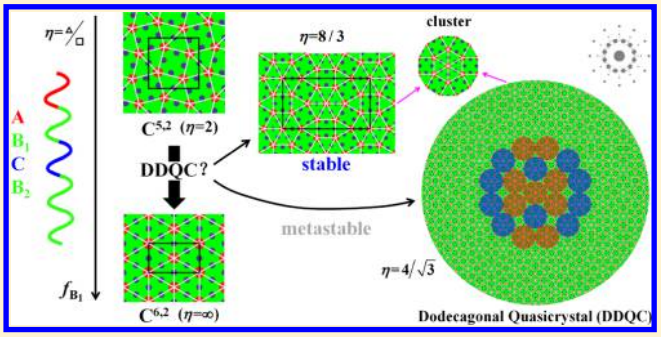

INTRODUCTION

Quasicrystals (QCs) are an interesting class of aperiodically ordered materials.[1,2] Since their discovery by Shechtman et al. in Al−Mn alloys in 1980s,[1] QCs have led to a redefinition of crystalline structures. Moreover, QC materials could have some interesting applications.[3] Therefore, QC has attracted tremendous attention from a wide range of fields.[4−6] Although QCs were initially observed in hard condensed matter systems, it has been shown that QCs could occur in a wide range of soft materials as well.[7−19] In particular, QC morphologies have been reported in self-assembling block copolymers (BCPs).[20−29] Despite numerous previous studies, a comprehensive and quantitative examination of the thermodynamic stability of QCs in BCPs has been lacking due to the difficulty originating from the aperiodicity of the structures.

BCPs are macromolecules composed of covalently linked and chemically distinct subchains or blocks. It has been well established that BCPs exhibit unique self-assembly behaviors,[30−42] thus providing opportunities for the formation of QC phases. Actually, in 1980, Leibler briefly considered the possibility of 5-fold symmetry in BCPs but dismissed it as not feasible.[43] Experimentally, Hayashida et al. observed an aperiodic morphology in blends of ISP-star terpolymers, where I, S, and P denote polyisoprene, polystyrene, and poly(2-vinylpyridine) blocks, respectively. This morphology was designated as a dodecagonal quasicrystal (DDQC).[21] Structurally, the DDQC morphology could be regarded as a specific tiling pattern composed of triangles and squares. A quasicrystalline tiling pattern can vary from an energetically stabilized ideal tiling pattern to an entropically stabilized random tiling pattern.[44] The ideal tiling DDQC structure tiled by triangles and squares subjects to a specific self-similarity rule, namely, the Stampfli inflation rule,[45−47] while in entropically stabilized QCs the entropy mainly stems from the dynamic rearrangement of subunits at high temperatures.[46,47] Thus, the periodicity is destroyed due to the maximization of the arrangement entropy of square and triangular subunits. In other words, there are many nearly degenerate arrangements leading to a more stable quasicrystalline state than the crystalline state.[4] For the DDQC structures, the ratio $\eta = N_T/N_S$ of the numbers of triangles (N_T) and squares (N_S) as an important characteristic parameter is an irrational number of $\eta = 4/\sqrt{3} \approx 2.309$. In the experiment by Hayashida et al.,[21] $\eta \approx 2.305$, very close to $4/\sqrt{3}$, was regarded as important evidence for the observation of the random DDQC pattern. In addition, the DDQC morphologies were also observed in a series of experiments by Bates and coworkers but were believed to be most likely metastable in their systems.[25−29]

Received: July 31, 2018
Revised: September 10, 2018
Published: September 24, 2018

DOI: 10.1021/acs.macromol.8b01638
Macromolecules 2018, 51, 7713−7721

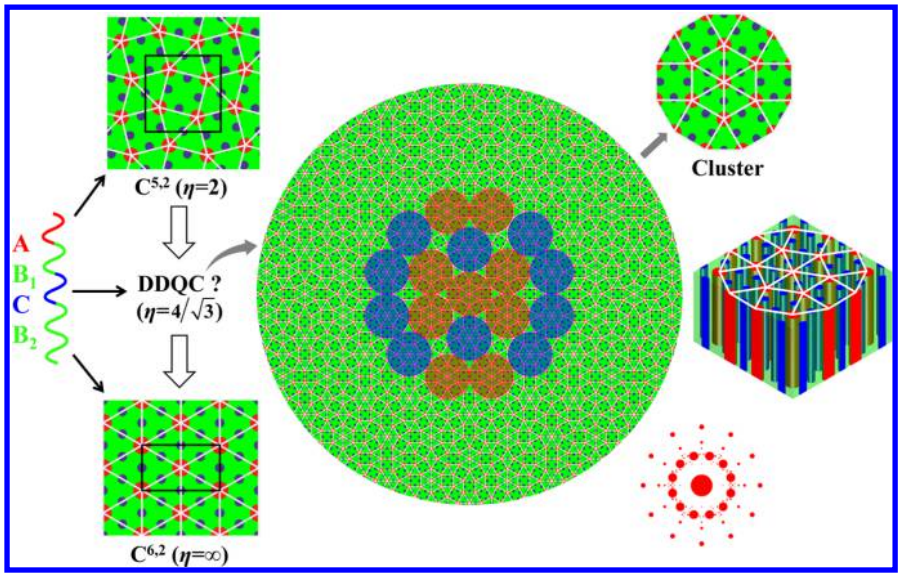

Figure 1. Illustration of the formation of dodecagonal quasicrystalline (DDQC) morphologies in the parameter space intermediate between two constituent periodic phases, $C^{5,2}$ and $C^{6,2}$, in AB_1CB_2 tetrablock terpolymer melts. Domains aggregated by the A and C blocks are plotted in red and blue, respectively, while the matrix of B blocks is plotted in green. White lines connecting neighboring A domains construct the DDQC lattice, which is composed of dodecagonal clusters with two possible orientations indicated by blue and orange shadowing circles, respectively. Isolated cluster is shown at the top right corner, a three-dimensional morphology with transparent B matrix is shown at the middle right, and the Fourier transform pattern of A domains in DDQC is shown at the bottom right corner.

The experimental observation of DDQC morphologies in various BCP systems presents a challenge to polymer theory. It is therefore desirable to extend the well-established theoretical framework of self-consistent field theory (SCFT)[48−50] to the study of QC order in inhomogeneous polymeric systems. In this work, we focus on the SCFT study of the stability of DDQC morphologies in BCP melts. In order to make progress on this topic, two critical problems, i.e., choosing a polymeric system and accurately determining the free energy of DDQC morphologies, need to be solved.

In order to choose a proper BCP system for the study we consider the fact that there are an infinite number of two-dimensional periodic tilings with triangles and squares. Among these tilings, two typical periodic tilings with $\eta = 2$ and ∞ are of particular interest (Figure 1). In particular, an ideal DDQC morphology consists of these two phases as substructures. Therefore, it is desirable to choose a BCP system that could form the two periodic phases. In order to examine the stability of different phases, the free energy of these phases needs to be determined accurately. It is noted that the accurate spectral method formulated in a higher dimensional space could be used to describe QC structures;[51] however, extending the spectral method of QCs to the SCFT has not been successful. Therefore, it is desirable to develop an efficient scheme of SCFT for the calculation of free energy of aperiodic DDQC structures.

The above argument motivates us to re-examine some of the previous work by Li's group on the self-assembly of purposely designed multiblock copolymers.[52] In particular, a sequence of cylindrical phases (denoted by $C^{m,n}$ with m and n indicating the coordination numbers (CNs) of A and C cylinders, respectively), $C^{4,2} \rightarrow C^{5,2} \rightarrow C^{6,2} \rightarrow C^{6,3}$, is predicted to form from the asymmetric AB_1CB_2 tetrablock terpolymers. It is important to note that the $C^{5,2}$ ($\eta = 2$) and $C^{6,2}$ ($\eta = \infty$) phases are exactly the constituent substructures of the ideal DDQC. Therefore, this terpolymer sample provides a proper candidate system for the study of DDQC. What is particularly useful is the fact that the CNs could be regulated by the copolymer compositions, thus providing an effective mechanism to consistently adjust the triangle/square ratio η of the different stable phases because η is closely related to the CNs (Table S1, Supporting Information including Tables S1−S7 and Figures S1−S4).

In this study, we aim to develop a combination method based on the self-consistent field theory for the study on the thermodynamic stability of dodecagonal structures. In order to make the computational cost as low as reasonable, we focus on the two-dimensional cylindrical DDQC structures with both ideal and random tiling patterns formed by judiciously tailored ABCB tetrablock terpolymer melts. First, we adopt the Stampfli inflation rule to generate a series of periodic DDQC approximants with the range of η value covering that of the ideal DDQC phase. Then, we use the SCFT to calculate the free energy of these DDQC approximants as well as other candidate phases and thus to determine their stabilities. Finally, we develop a semianalytical cluster model to analyze the relative stabilities between these DDQC approximants so that we could predict the stability of aperiodic DDQC structures.

■ THEORY AND METHODS

We consider an incompressible melt of n linear AB_1CB_2 tetrablock terpolymer chains with the total number of segments N in a volume of V. The length of each block is specified by f_AN, $f_{B_1}N$, f_CN, and $f_{B_2}N$, with $f_{B_1} + f_{B_2} = f_B$ and $f_A + f_B + f_C = 1$. The interaction parameters are fixed as $\chi_{AB}N = \chi_{BC}N = \chi_{AC}N = \chi N = 80$ except where otherwise specifically indicated, where χ_{ij} is the Flory−Huggins parameter characterizing the immiscibility between monomers i and j. Generally, we assume that all polymers have equal Kuhn length b and segment density ρ_0. Within the standard SCFT based on the Gaussian-chain model,[49,53] the free energy per chain in the unit of thermal energy k_BT for a given temperature T, where k_B is the Boltzmann constant, can be expressed as

DOI: 10.1021/acs.macromol.8b01638
Macromolecules 2018, 51, 7713−7721

$$f = \frac{F}{nk_BT} = -\ln Q + \frac{1}{V}\int d\mathbf{r}\left\{\frac{1}{2}\sum_i\sum_{j\neq i}\chi_{ij}N\phi_i(\mathbf{r})\phi_j(\mathbf{r}) - \sum_i w_i(\mathbf{r})\phi_i(\mathbf{r}) - \xi(\mathbf{r})\left[1 - \sum_i \phi_i(\mathbf{r})\right]\right\},\ (i, j = \mathrm{A,B,C}) \quad (1)$$

where $\phi_i(\mathbf{r})$ is the volume fraction function of monomer i and $w_i(\mathbf{r})$ denotes its conjugate mean field (i = A, B, C). The spatial function $\xi(\mathbf{r})$ is a Lagrange multiplier used to enforce the incompressibility conditions, $\phi_A(\mathbf{r}) + \phi_B(\mathbf{r}) + \phi_C(\mathbf{r}) = 1$. The quantity Q is the partition function of the single terpolymer chain interacting with the mean fields of $w_i(\mathbf{r})$ (i = A, B, C), which is determined by

$$Q = \frac{1}{V}\int d\mathbf{r} q(\mathbf{r}, s)q^\dagger(\mathbf{r}, s) \quad (2)$$

Here $q(\mathbf{r},s)$ and $q^\dagger(\mathbf{r},s)$ are the propagator functions of segments starting from the two ends, respectively, satisfying the following modified diffusion equations

$$\frac{\partial q(\mathbf{r}, s)}{\partial s} = \nabla^2 q(\mathbf{r}, s) - w(\mathbf{r}, s)q(\mathbf{r}, s)$$
$$-\frac{\partial q^\dagger(\mathbf{r}, s)}{\partial s} = \nabla^2 q^\dagger(\mathbf{r}, s) - w(\mathbf{r}, s)q^\dagger(\mathbf{r}, s) \quad (3)$$

where $w(\mathbf{r},s) = w_i(\mathbf{r})$ when s belongs to the i component blocks along the polymer chain. The above expressions imply that $R_g = (N/6)^{1/2}b$ is chosen as the unit of spatial length. The initial conditions of the propagator functions are $q(\mathbf{r},0) = q^\dagger(\mathbf{r},1) = 1$. Minimization of the free energy with respect to the volume fraction functions and the mean fields leads to the following SCFT equations

$$w_i(\mathbf{r}) = \xi(\mathbf{r}) + \sum_{j\neq i}\chi_{ij}N\phi_j(\mathbf{r}) \quad (4)$$

$$\phi_A(\mathbf{r}) = \frac{1}{Q}\int_0^{f_A} ds q(\mathbf{r}, s)q^\dagger(\mathbf{r}, s),$$
$$\phi_B(\mathbf{r}) = \frac{1}{Q}\left[\int_{f_A}^{f_A+f_{B_1}} ds q(\mathbf{r}, s)q^\dagger(\mathbf{r}, s) + \int_{1-f_{B_2}}^{1} ds q(\mathbf{r}, s)q^\dagger(\mathbf{r}, s)\right],$$
$$\phi_C(\mathbf{r}) = \frac{1}{Q}\int_{f_A+f_{B_1}}^{1-f_{B_2}} ds q(\mathbf{r}, s)q^\dagger(\mathbf{r}, s) \quad (5)$$

$$0 = 1 - \sum_i \phi_i(\mathbf{r}),\ (i, j = \mathrm{A, B, C}) \quad (6)$$

The modified diffusion equations are solved using the pseudospectral method[54] with periodic boundary conditions imposed on all directions, and Anderson mixing iteration[55] is implemented to accelerate the converging speed toward SCFT solutions. The chain contour is divided into 200 points, i.e., $\Delta s = 5 \times 10^{-3}$. The terpolymer melts are placed in a two-dimensional rectangular box with sizes $L_x \times L_y$, which is divided into a grid lattice of $N_x \times N_y$. To ensure a reliable accuracy, the grid size is chosen such that the grid spacing $\Delta x = L_x/N_x$ or $\Delta y = L_y/N_y$ smaller than $0.1R_g$. Note that the free energy of each candidate ordered phase is minimized with respect to the box sizes L_x and L_y during our SCFT calculations.

RESULTS AND DISCUSSION

Stampfli Inflation Rule. To circumvent the computational difficulty due to the aperiodicity of DDQC, we adopt the Stampfli inflation rule[45−47] to generate a sequence of periodic DDQC approximants, of which the ith generation is designated by QC-G$_i$. Although the DDQC approximants of any generation are periodic, the boundary effects decrease rapidly as the number of generation is increased.[47] The number of triangles and squares of QC-G$_i$ is determined by a recursion relation[46,47]

$$\begin{bmatrix} N_T^{(i)} \\ N_S^{(i)} \end{bmatrix} = \begin{bmatrix} 7 & 16 \\ 3 & 7 \end{bmatrix}\begin{bmatrix} N_T^{(i-1)} \\ N_S^{(i-1)} \end{bmatrix} \quad (7)$$

with initial condition $[N_T^0, N_S^0] = [0, 1]$, where N_T^i and N_S^i indicate the number of triangles and squares contained in the unit cell of QC-G$_i$, respectively. For instance, $\eta^{(1)} = N_T^{(1)}/N_S^{(1)} = 16/7 \approx 2.2857$ for QC-G$_1$. $\eta^{(2)} = N_T^{(2)}/N_S^{(2)} = 224/97 \approx 2.3093$ for QC-G$_2$, which is surprisingly already very close to the ideal value of 2.3094.

For QC-G$_2$, the cell size L is as large as $63R_g$, around 1 μm for a moderate molecular weight of polymer. Additionally, the Fourier transform pattern of QC-G$_2$ exhibits the main peaks of ideal DDQC (Figure 1). In our SCFT calculations, the grid lattice for QC-G$_2$ is set as $N_x \times N_y = 768 \times 768$, of which the calculation labor is affordable for nowadays computer. However, for QC-G$_3$, $L_x = L_y$ becomes $(2 + \sqrt{3})$ times larger, thus requiring the grid lattice as large as $N_y \times N_y = 3072 \times 3072$. Therefore, the computational cost for QC-G$_3$ becomes extremely high.

Phase Diagrams. As mentioned above, our previous work has predicted the phase sequence of $C^{4,2} \rightarrow C^{5,2} \rightarrow C^{6,2} \rightarrow C^{6,3}$ in the AB_1CB_2 melts with $0.12 < f_A = f_C < 0.14$ but with a negligibly tiny region of $C^{6,2}$.[52] It has been established that the phase transitions between those mesocrystals in the linear terpolymers are governed by two principles.[52] The first principle is that the average CN ($C\bar{N}$) decreases as the bridging middle B_1 block shortens. The second principle is that the asymmetry of the molecular architectures dictates the asymmetry of CNs. The presence of $C^{6,2}$ ($C\bar{N} = 3$) between $C^{5,2}$ ($C\bar{N} = 20/7$) and $C^{6,3}$ ($C\bar{N} = 4$) follows the first principle but violates the second one because the CN asymmetry of $C^{6,2}$ is larger than those of the two others, thus resulting in the narrow region of $C^{6,2}$. Therefore, the stability region of $C^{6,2}$ could be widened by simply enlarging the molecular asymmetry, e.g., changing the symmetric composition $f_A = f_C$ to be asymmetric $f_A > f_C$.[52]

We examine the stability of the DDQC structures by two steps. First, we construct the phase diagrams by considering a series of representative periodic phases composed of triangles and squares.[56] It is well known that the completeness of a phase diagram relies critically on the library of candidate phases. However, it is impossible to exhaust all triangle/square tilings. Therefore, in the second step, we attempt to probe into the mechanisms governing the relative stabilities of these candidate phases and then to predict the possibilities for other phases to become stable, particularly focusing on the periodic DDQC approximants and aperiodic DDQC morphologies. Besides the phases of $C^{4,2}$, $C^{5,2}$, $C^{6,2}$, $C^{6,3}$, H phase, QC-G$_1$ and QC-G$_2$, four more morphologies are considered, which are denoted as QC-APX$_i$ (i = 1, 2, 3, 4) with η (= 2.2857, 2.3333, 2.4, 2.6667), intermediate between $\eta = 2$ of $C^{5,2}$ and $\eta = \infty$ of $C^{6,2}$ (Table S1). Apparently, this range of η of QC-APX$_i$ covers $\eta \approx 2.3094$ of the ideal DDQC.

The phase diagram in the f_{B_1}−f_C plane for a fixed $f_A = 0.14$ is shown in Figure 2a. As expected, the $C^{6,2}$ exhibits a

DOI: 10.1021/acs.macromol.8b01638
Macromolecules 2018, 51, 7713−7721

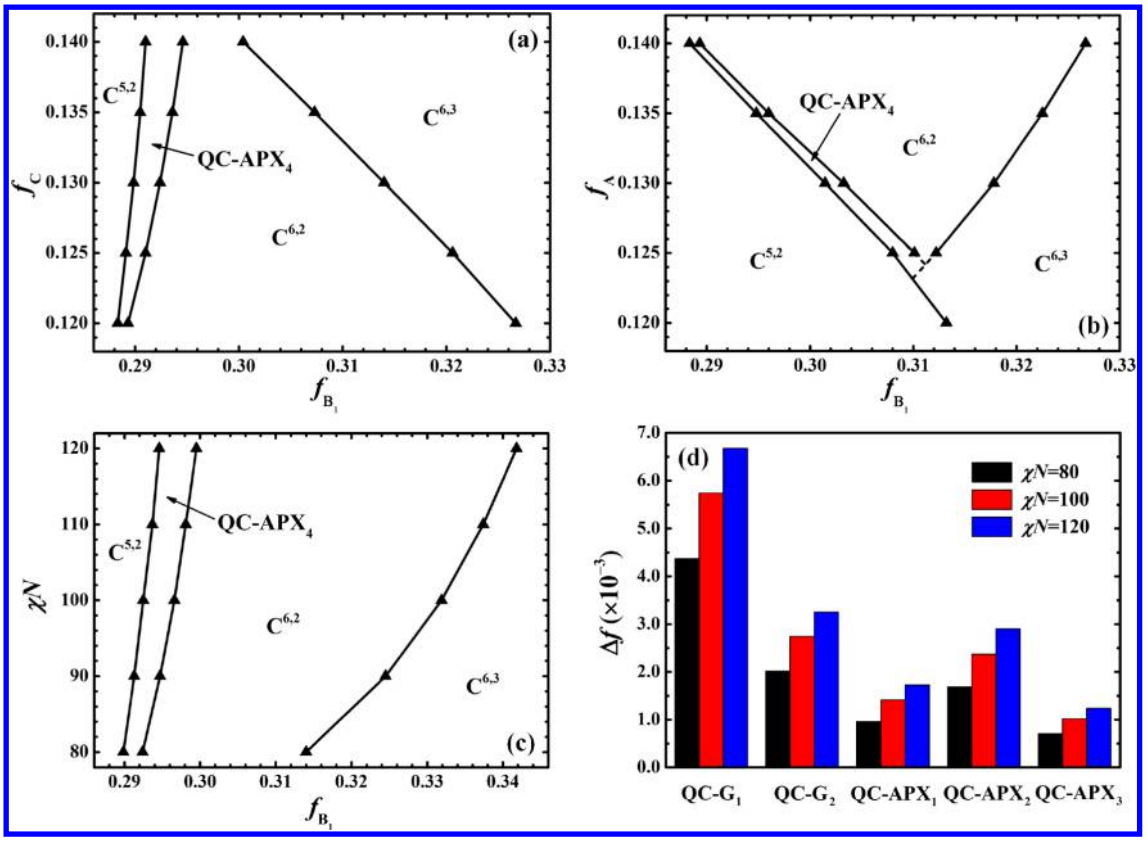

Figure 2. Phase diagrams for AB_1CB_2 terpolymers (a) in the f_{B_1}–f_C plane with $f_A = 0.14$ and $\chi N = 80$, (b) in the f_{B_1}–f_A plane with $f_C = 0.12$ and $\chi N = 80$, and (c) in the f_{B_1}–χN plane with $f_A = 0.14$ and $f_C = 0.13$. Symbols indicate the transition points determined by SCFT, while solid lines are a guide for the eyes. (d) Free energy difference $\Delta f = f - f_{QC\text{-}APX4}$ for DDCPs with $f_A = 0.14$ and $f_C = 0.13$ at the $C^{5,2}/C^{6,2}$ phase boundaries for $\chi N = 80$, 100, and 120.

considerable stable region between $C^{5,2}$ and $C^{6,3}$ when $f_A > f_C$. Detailed free energy comparison between the different candidate phases is given in Figure S1. A surprising result is that the QC-APX_4 structure exhibits a noticeable stability window intermediate between $C^{5,2}$ and $C^{6,2}$, but QC-G_2 is metastable. In addition, similar results are observed with the phase diagram in the f_{B_1}–f_A plane for $f_C = 0.12$ (Figure 2b). It is also interesting to note that the phase region of QC-APX_4 can be expanded by increasing χN (Figure 2c).

An important result from the study is that a general transition sequence is predicted from the phase diagrams, e.g., $C^{5,2} \rightarrow$ QC-APX_4 $\rightarrow C^{6,2}$, which obviously follows the regulation principle of the adjustable bridge B_1 block (Figure 3).[S2] However, the absence of the phases with the value of η intermediate between $\eta = 2$ of $C^{5,2}$ and $\eta = 2.6667$ of QC-APX_4 could not be rationalized by this principle, such as QC-APX_1/QC-G_1 with $\eta = 2.2857$, QC-G_2 with $\eta = 2.3093$, QC-APX_2 with $\eta = 2.3333$ and QC-APX_3 with $\eta = 2.4$. Therefore, more sophisticated interpretations are needed for their relative stabilities. Interestingly, these phases share a common structural feature as DDQC, i.e., that they are mainly composed of identical dodecagonal clusters, each of which is comprised of 12 triangles and 6 squares (Tables S2 and S3). Accordingly, they can be classified as DDQC approximants that exhibit similar scattering profiles as that of the aperiodic DDQC structure (Table S1). For convenience, these DDQC approximants are referred to as dodecagonal cluster phases (DDCPs).

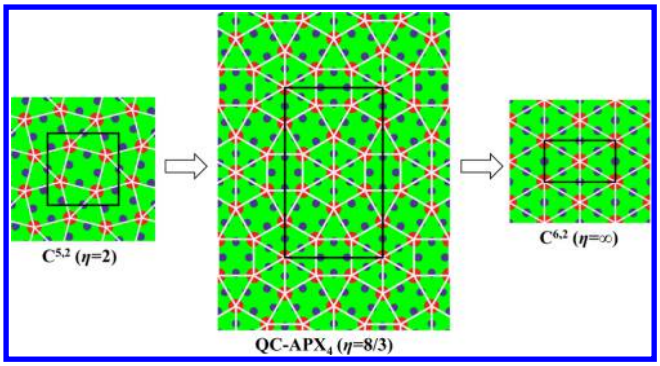

Figure 3. Density plots of the general sequence of stable phases observed in the considered ABCB terpolymer systems, i.e., $C^{5,2} \rightarrow$ QC-APX_4 $\rightarrow C^{6,2}$ with corresponding η value.

It is important to note that the free energy differences between these DDCPs change very mildly in the region of $0.285 \leq f_{B_1} \leq 0.3$ (Figure S1e). This observation implies that the relative stabilities between these phases are dictated by some intrinsic and delicate factor, which may originate from their geometrical tilings. Therefore, we could examine the relative stabilities of these DDCPs as well as other possible DDCPs including ideal and random tiling DDQC patterns by focusing on a specific phase point within the region of QC-APX_4, e.g., the $C^{5,2}/C^{6,2}$ transition point for $f_A = 0.14$ and $f_C = 0.13$ in Figure 2a. The free energies relative to that of QC-APX_4 are presented in Figure 2d. In addition, the free energies

DOI: 10.1021/acs.macromol.8b01638
Macromolecules 2018, 51, 7713−7721

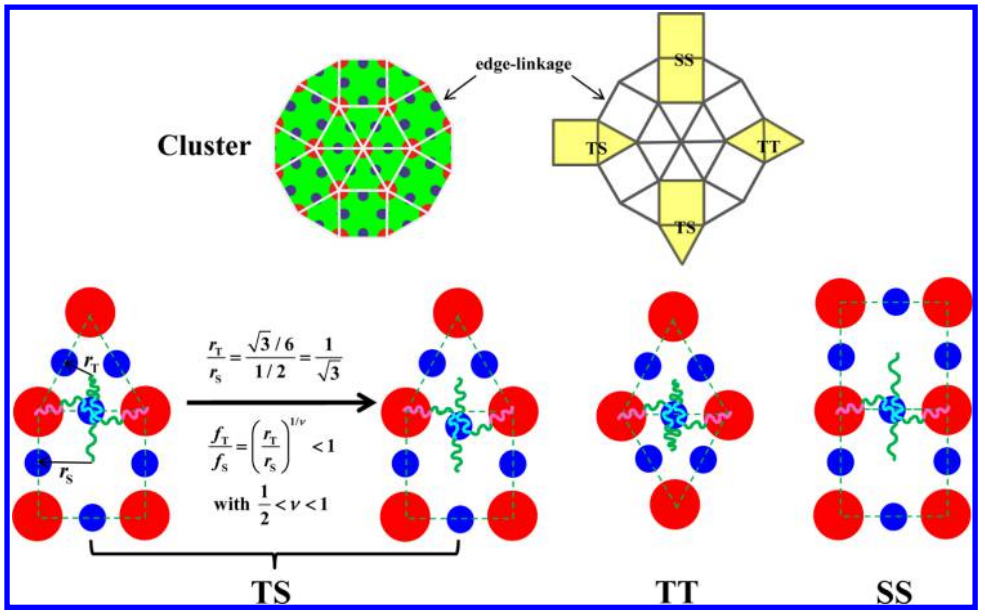

Figure 4. Illustration of different packing frustrations of the tail B_2 blocks in edge linkages with TS, TT, and SS types for one dodecagonal cluster.

for χN = 100 and 120 are calculated, indicating that the relative stabilities of these DDCPs are insensitive to the value of χN. It is necessary to note that the segregation with the values of 80 $\leq \chi N \leq$ 120 is intermediate for the tetrablock copolymers. According to the dependence of the phase boundaries on the value of χN in Figure 2c, the conclusion about the relative stabilities between these DDCPs should also hold for the strong segregation region (low temperature). This observation further confirms that their relative stabilities should stem from the different arrangements of triangles and squares.

Cluster Model. It has been established that the stability or metastability of QC in hard materials originates from electronic structures.[4] In contrast, the formation of ordered phases in BCPs is dictated by the competition between the interfacial energy and the chain stretching entropy, usually leading to the packing frustration of polymer chains.[57,58] Here we will elucidate the critical role of packing frustration closely related to the lattice mismatch on the metastability of DDQC based on the following observations (Figure 4). For the tiling patterns composed of squares and triangles, there are only three possible types of linkages, namely, triangle−triangle (TT), triangle−square (TS), and square−square (SS) (Figure 4). For the TS linkage, the tail B_2 blocks are more stretched in the square than in the triangle, causing the packing frustration (Figure 4). This is because the ratio of distances from the C domain on the linkage to the center of the square is larger than that of the triangle, leading to highly different stretching degrees of B_2 blocks in the two subunits (i.e., packing frustration). To release this frustration, the C domains are pushed away from the linkage toward the center of the square. On the other hand, it is important to note that the lattice constant a, the equilibrium distance between neighboring A domains, in the phase of lower $C\bar{N}$ is smaller for the same parameters,[52] e.g., $a(C^{4,2}) < a(C^{5,2}) < a(C^{6,2})$ (Figure S2). Similarly, the lattice constants of the DDCPs are intermediate between those of the two constituent phases of $C^{5,2}$ and $C^{6,2}$ but very close to that of $C^{5,2}$ mainly consisting of TS pairs. Therefore, the TS linkage in DDCPs is a favorable configuration. In contrast, both the TT and the SS linkages are energetically unfavorable because they are compressed and expanded relative to their native lattice constants in $C^{6,2}$ and $C^{4,2}$, thus leading to extra compression and stretching to the tail blocks, respectively (Figure 4). However, as the TT linkage comprises the hexagonal lattice with the minimal packing frustration, its energy cost is less than that of the SS linkage. In a word, the TS linkage is most beneficial to the stability of DDCPs while the SS linkage is the worst.

To quantitatively determine the energy penalty from the TT and SS linkages, a cluster model is developed based on ideas from the hard QCs.[4,59] DDCPs are composed of identical dodecagonal clusters in contact or overlapped, and their interstitial space if existing is filled by some triangles or squares (Table S2). In other words, each cluster interacts with others or with the environment via various "edge linkages" (Figure 4), each of which is formed by its peripheral triangle/square with another triangle/square in the neighboring cluster or in the interstitial space. As discussed above, there are three possible types of linkages (i.e., TT, TS and SS), which exhibit different packing frustrations (Figure 4), thus having distinct energy costs. As a result, the small free energy difference between different DDCPs mainly originates from the different edge linkages on their clusters. On the basis of the above argument, a simple derivation is given as follows.

The contribution of every isolated cluster to the free energy is rarely influenced by the environment and thus is nearly constant, f_0, particularly for the DDCPs composed of nonoverlapped clusters. On average, the free energy of one DDCP is dictated by the average number of α linkages per cluster, $\bar{n}_\alpha$. Within such single-cluster approximation, the volume density of free energy of one DDCP can be written as

$$f = f_0 + \frac{N\rho_0^{-1}}{k_B T V_{\text{cluster}}} \sum_\alpha K_\alpha \bar{n}_\alpha, \left(\sum_\alpha \bar{n}_\alpha = 12, \alpha = \text{TT, TS, SS} \right) \tag{8}$$

where V_{cluster} indicates the cluster volume and K_α quantifies the energy cost of one α linkage. Obviously, eq 8 ignores higher order correlations between the clusters. Then we can rewrite eq 8 into $f = f'_0 + f^{\text{exc}}$, where the trivial term $f'_0 = f_0 +$

DOI: 10.1021/acs.macromol.8b01638
Macromolecules 2018, 51, 7713−7721

$12K_{TT}N\rho_0^{-1}/k_BTV_{cluster}$ contains f_0 and the reference energy from the 12 TT linkages and the excess term

$$f^{exc} = \kappa_{TS}\overline{n}_{TS} + \kappa_{SS}\overline{n}_{SS}, (6 \le \overline{n}_{TS} + \overline{n}_{SS} \le 12) \quad (9)$$

with $\kappa_{TS} = (K_{TS} - K_{TT})N\rho_0^{-1}/k_BTV_{cluster}$ and $\kappa_{SS} = (K_{SS} - K_{TT})N\rho_0^{-1}/k_BTV_{cluster}$ denoting the energy contributions by one TS linkage and one SS linkage relative to the TT linkage and $\overline{n}_{TS}$ and $\overline{n}_{SS}$ denote the average number of TS and SS linkages per cluster, respectively. Thus, we have $\kappa_{TS} < 0$ and $\kappa_{SS} > 0$ based on the qualitative analysis above.

Because of phason flip, various η-degenerate morphologies for DDCPs with different $\overline{n}_{TS}$ and $\overline{n}_{SS}$ could be generated, thus enabling one to estimate the coefficients of κ_{TS} and κ_{SS}. Specifically, κ_{TS} is estimated as $\kappa_{TS} \approx -2.9 \times 10^{-4}$ by linearly fitting the free energy differences between four η-degenerate morphologies of QC-APX$_2$ with different values of $\overline{n}_{TS}$ but $\overline{n}_{SS} = 0$ (Table S3, Figure S3). Then κ_{SS} is estimated as $\kappa_{SS} \approx 1.0-1.4 \times 10^{-3} \gg |\kappa_{TS}|$ from a few groups of η-degenerate morphologies using $\kappa_{TS} \approx -2.9 \times 10^{-4}$ and eq 9 (Table S4), which indicates the predominant role of SS pair on the relative stabilities of DDCPs.

Stability of Ideal Tiling DDQC. The cluster model can be used to compute the free energy differences between η-degenerate morphologies with a reliable accuracy by simply counting their differences in the average numbers of TS and SS linkages per cluster. Accordingly, we employ the cluster model to predict the lower limit of the free energy of QC-G$_2$ with the "optimal" arrangement of clusters, i.e., without any SS linkage. We generated 12 η-degenerate morphologies of QC-G$_2$ with different $\overline{n}_{TS}$ or $\overline{n}_{SS}$ (Table S5) and then calculate their free energies using SCFT. We plot the reduced free energy, $f' = f - \kappa_{TS}\overline{n}_{TS}$, as a function of $\overline{n}_{SS}$ or the total number N_{SS} of SS linkages in the unit cell (Figure 5). As predicted by the cluster model, the data points follow a linear relationship leading to $\kappa_{SS} \approx 1.02 \times 10^{-3}$. Moreover, those data points with the same value of $\overline{n}_{SS}$ overlap very well. A linear extrapolation gives rise to the lower limit of the trivial term of free energy $f'^* \approx 13.18676$ of QC-G$_2$ without SS linkages, which is nearly equal to $f' = 13.18675$ for the QC-APX$_4$. After including the contribution of the maximal number of TS linkages, the absolute value of free energy $f^* \approx 13.18328$ is still not lower than that of QC-APX$_4$, i.e., $f = 13.18327$. Though the ideal DDQC phase can be iteratively approached by increasing the generation number i of QC-G$_i$ in the Stampfli construction rule, to the best of our knowledge it is impossible to replace all of the SS and TT linkages with TS ones. Therefore, the limiting free energy obtained by extrapolation for QC-G$_2$ with $\overline{n}_{SS} = 0$ should be the lower limit of the free energy of ideal tiling DDQC phase.

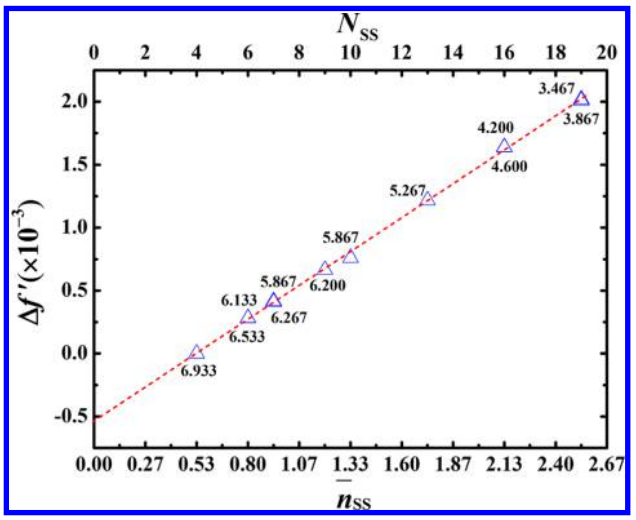

Figure 5. Reduced free energy f' of different QC-G$_2$ morphologies relative to that of QC-G$_2$ with $N_{SS} = 4$ as a function of $\overline{n}_{SS}$ or N_{SS} for $\chi N = 80$, $f_{B_1} = 0.292$, $f_A = 0.14$, and $f_C = 0.13$. Data around each symbol indicates its corresponding value of $\overline{n}_{TS}$. Linear extrapolation leads to the lower limit of free energy for $N_{SS} = 0$, $f'^* \approx 13.18676$.

The above discussions lead to an important conclusion that the ideal DDQC should be metastable in this terpolymer melt. Although the cluster model becomes less rigorous for the DDCPs with different values of η (e.g., QC-G$_1$, QC-G$_2$, QC-APX$_1$, and QC-APX$_2$) or with overlapped clusters (e.g., QC-APX$_3$ and QC-APX$_4$), it could provide a qualitative understanding on their relative stabilities by ranking $\overline{n}_{SS}$ and then $\overline{n}_{TS}$, i.e., their free energies in the descending order of QC-G$_1$ with $(\overline{n}_{SS}, \overline{n}_{TS}) = (2.0, 4.0)$, QC-G$_2$ with (0.533, 6.933), QC-APX$_2$ with (0, 6.0), QC-APX$_1$ with (0, 8.0), QC-APX$_3$ with (0, 10.0), and QC-APX$_4$ with (0, 12.0) (Table S2).

Stability of Random Tiling DDQC. In many soft matter systems the dodecagonal symmetry originates from tiling entropy.[4,6,24,47] However, in the self-assembly of block copolymer melts, the rearrangement entropy of the triangular/square subunits is overwhelmed by the configurational entropy of the polymer chains at a much smaller length scale (e.g., from Kuhn length to the radius of gyration). Thus, we only need to examine the energetic stabilities of random tiling DDQC morphologies.

We constructed 8 different random tiling morphologies via the zipper and connectivity update moves over different QC-G$_2$ patterns (Figure 6 and Table S6)[47] and calculated their free energies. We find that these random tiling morphologies are rather less stable than the QC-G$_2$ morphology with $N_{SS} = 4$ (Figure 7). Obviously, the cluster model is not suitable for the random tiling morphologies because they are not mainly composed of the dodecagonal clusters. However, fortunately, the number of SS pairs is still a good quantity accounting for their relative stabilities because the SS linkage causes the most energy penalty (Figure 7).

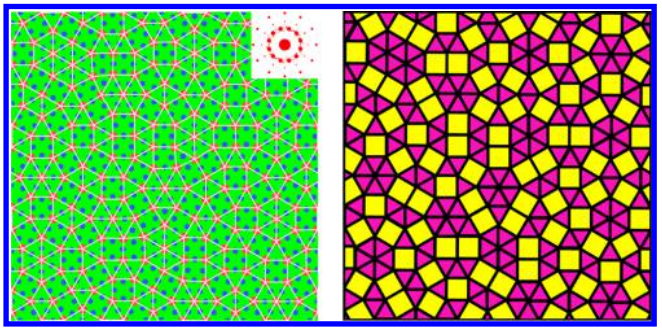

Figure 6. One random tiling morphology with $N_{SS} = 18$ from the second-generation DDQC approximant QC-G$_2$ and others are shown in Table S6. (Left) Density plot with the Fourier transform pattern shown in the top-right corner. (Right) Corresponding tiling pattern of the triangles (yellow) and squares (pink).

There seems be no possibility for random tiling morphologies to be more stable than QC-APX$_4$ because of the large number of SS pairs.[47,56] However, there exists

DOI: 10.1021/acs.macromol.8b01638
Macromolecules 2018, 51, 7713−7721

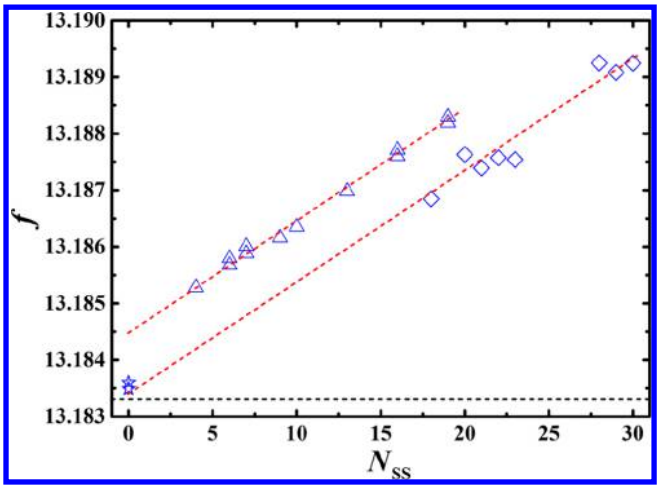

Figure 7. Free energy per chain as a function of N_{SS} for $\chi N = 80$, $f_{B1} = 0.292$, $f_A = 0.14$, and $f_C = 0.13$. Unfilled triangles and diamonds indicate the free energies of the ideal (list in Table S5) and random tiling morphologies from zipper update (list in Table S6), respectively, while the unfilled stars indicate that of the coexistence patterns of $C^{5,2}$/QC-APX_4 without SS-pairs (list in Table S7). Red dashed lines show the changing trend of the free energies for the ideal and random morphologies, and horizontal dashed line indicates the free energy of QC-APX_4.

another kind of random tiling pattern without energy-expensive SS pairs, which can be constructed by epitaxially piecing together the substructures of $C^{5,2}$ and QC-APX_4. This kind of morphology can be regarded as the mesoscopic coexistence of the $C^{5,2}$ and QC-APX_4 phases. This is reminiscent of the random DDQC patterns observed in the blend of ABC miktoarm star copolymers by experiment.[21] Here we try to make a heuristic exploration for this kind of pattern by constructing several $C^{5,2}$/QC-APX_4 coexistence morphologies with η values covering that of DDQC (Table S7). Their free energies calculated on the $C^{5,2}$/QC-APX_4 transition point are slightly higher than that of QC-APX_4 with the free-energy difference per chain from $1.8 \times 10^{-4} k_B T$ to $2.9 \times 10^{-4} k_B T$ (Figure S4). Hence, it is reasonable to speculate that the stable random tiling pattern of $C^{5,2}$/QC-APX_4 coexistence could be observed in judiciously designed blends of different block copolymers.

CONCLUSIONS

In this work, the formation of two-dimensional cylindrical DDQC approximants in ABCB terpolymer melts is studied by SCFT. Both the ideal and the random tiling DDQC morphologies are predicted to be metastable, whereas a DDQC approximant of QC-APX_4 is stable. For the ideal tiling DDQC, a cluster model is developed revealing quantitatively that the relative stabilities of the DDQC morphologies and approximants are mainly dictated by the packing frustration of polymer chains presented in the compressed triangle−triangle and expanded square−square pairs. For the random tiling DDQC it is suggested that the coexistence pattern of $C^{5,2}$/QC-APX_4 could be stable in block copolymer blends. Three important conclusions could be drawn from the current study. First, the observation of the stable QC-APX_4 is significant for experiments because this structure is hard to be distinguished from the ideal DDQC morphology. Second, the revealed mechanism not only deepens the understanding of the formation of DDQC morphologies but also provides designing rules for new systems to form stable DDQC morphologies. Third, there is a considerable possibility to experimentally observe a metastable two-dimensional DDQC morphology considering that the free energy of DDQC is only slightly higher than that of the stable phase.

Whether our conclusion applies to the case of three-dimensional spherical structures[25−29] is obviously another important question. In the three-dimensional system, there is the third dimension to release the packing frustration within the most energetically expensive SS pair, thus reducing its energy penalty. As a result, there might be a high possibility to observe three-dimensional spherical DDQC structures. Nevertheless, this work provides a useful guide for experiments to distinguish the DDQC morphologies from the DDQC approximants or their mesoscopic coexistence morphologies.

ASSOCIATED CONTENT

Supporting Information

The Supporting Information is available free of charge on the ACS Publications website at DOI: 10.1021/acs.macromol.8b01638.

List of considered two-dimensional candidate phases, tiling patterns of six different dodecagonal cluster phases, list of several η-degenerate tiling patterns of QC-APX_2, free energy per chain and average number of TS and SS linkages per cluster for two groups of phases, number of η-degenerate tiling patterns of QC-G_2, number of η-degenerate tiling patterns of random tiling DDQC, several periodic $C^{5,2}$/QC-APX_4 coexistence patterns, typical free energy comparison among considered ordered phases, comparisons of lattice constant a for considered ordered phases, free energy per chain of a few η-degenerate morphologies of QC-APX_2, and free energy comparison of several $C^{5,2}$/QC-APX_4 coexistence morphologies (PDF)

AUTHOR INFORMATION

Corresponding Author

*E-mail: weihuali@fudan.edu.cn.

ORCID

Weihua Li: 0000-0002-5133-0267

An-Chang Shi: 0000-0003-1379-7162

Author Contributions

‡C.D., M.Z., and Y.Q.: These authors contributed equally.

Notes

The authors declare no competing financial interest.

ACKNOWLEDGMENTS

This work was supported by the National Natural Science Foundation of China (Grants Nos. 21574026 and 21774025). A.-C.S. acknowledges support from the Natural Science and Engineering Research Council (NSERC) of Canada.

REFERENCES

(1) Shechtman, D.; Blech, I.; Gratias, D.; Cahn, J. W. Metallic Phase with Long-Range Orientational Order and No Translational Symmetry. *Phys. Rev. Lett.* **1984**, *53*, 1951.

(2) Levine, D.; Steinhardt, P. J. Quasicrystals: A New Class of Ordered Structures. *Phys. Rev. Lett.* **1984**, *53*, 2477−2480.

(3) Dubois, J. M. *Useful Quasicrystals*; World Scientific, 2003.

(4) DiVincenzo, D.; Steinhardt, P. *Quasicrystals: The State of the Art*; World Scientific, 1999.

DOI: 10.1021/acs.macromol.8b01638
Macromolecules 2018, 51, 7713−7721

(5) Steurer, W. Twenty Years of Structure Research on Quasicrystals. *Z. Kristallogr. - Cryst. Mater.* **2004**, *219*, 391−446.
(6) Steurer, W. Why Are Quasicrystals Quasiperiodic? *Chem. Soc. Rev.* **2012**, *41*, 6719−6729.
(7) Zeng, X. B.; Ungar, G.; Liu, Y. S.; Percec, V.; Dulcey, A. E.; Hobbs, J. K. Supramolecular Dendritic Liquid Quasicrystals. *Nature* **2004**, *428*, 157−160.
(8) Mikhael, J.; Roth, J.; Helden, L.; Bechinger, C. Archimedean-Like Tiling on Decagonal Quasicrystalline Surfaces. *Nature* **2008**, *454*, 501−504.
(9) Talapin, D. V.; Shevchenko, E. V.; Bodnarchuk, M. I.; Ye, X. C.; Chen, J.; Murray, C. B. Quasicrystalline Order in Self-Assembled Binary Nanoparticle Superlattices. *Nature* **2009**, *461*, 964−967.
(10) Fischer, S.; Exner, A.; Zielske, K.; Perlich, J.; Deloudi, S.; Steurer, W.; Lindner, P.; Förster, S. Colloidal Quasicrystals with 12-Fold and 18-Fold Diffraction Symmetry. *Proc. Natl. Acad. Sci. U. S. A.* **2011**, *108*, 1810−1814.
(11) Iacovella, C. R.; Keys, A. S.; Glotzer, S. C. Self-Assembly of Soft-Matter Quasicrystals and Their Approximants. *Proc. Natl. Acad. Sci. U. S. A.* **2011**, *108*, 20935−20940.
(12) Reinhardt, A.; Romano, F.; Doye, J. P. K. Computing Phase Diagrams for a Quasicrystal-Forming Patchy-Particle System. *Phys. Rev. Lett.* **2013**, *110*, 255503.
(13) Dotera, T.; Oshiro, T.; Ziherl, P. Mosaic Two-Lengthscale Quasicrystals. *Nature* **2014**, *506*, 208−211.
(14) Barkan, K.; Engel, M.; Lifshitz, R. Controlled Self-Assembly of Periodic and Aperiodic Cluster Crystals. *Phys. Rev. Lett.* **2014**, *113*, 098304.
(15) Yue, K.; et al. Geometry Induced Sequence of Nanoscale Frank-Kasper and Quasicrystal Mesophases in Giant Surfactants. *Proc. Natl. Acad. Sci. U. S. A.* **2016**, *113*, 14195−14200.
(16) Dotera, T.; Bekku, S.; Ziherl, P. Bronze-Mean Hexagonal Quasicrystal. *Nat. Mater.* **2017**, *16*, 987−992.
(17) Ye, X. C.; Chen, J.; Irrgang, M. E.; Engel, M.; Dong, A. G.; Glotzer, S. C.; Murray, C. B. Quasicrystalline Nanocrystal Superlattice with Partial Matching Rules. *Nat. Mater.* **2017**, *16*, 214−219.
(18) Sun, Y.; Ma, K.; Kao, T.; Spoth, K. A.; Sai, H.; Zhang, D.; Kourkoutis, L. F.; Elser, V.; Wiesner, U. Formation Pathways of Mesoporous Silica Nanoparticles with Dodecagonal Tiling. *Nat. Commun.* **2017**, *8*, 252.
(19) Zu, M. J.; Tan, P.; Xu, N. Forming Quasicrystals by Monodisperse Soft Core Particles. *Nat. Commun.* **2017**, *8*, 2089.
(20) Dotera, T. Mean-field Theory of Archimedean and Quasicrystalline Tilings. *Philos. Mag.* **2007**, *87*, 3011−3019.
(21) Hayashida, K.; Dotera, T.; Takano, A.; Matsushita, Y. Polymeric Quasicrystal: Mesoscopic Quasicrystalline Tiling in ABC Star Polymers. *Phys. Rev. Lett.* **2007**, *98*, 195502.
(22) Lee, S.; Bluemle, M. J.; Bates, F. S. Discovery of a Frank-Kasper σ Phase in Sphere-Forming Block Copolymer Melts. *Science* **2010**, *330*, 349−353.
(23) Matsushita, Y.; Hayashida, K.; Dotera, T.; Takano, A. Kaleidoscopic Morphologies from ABC Star-shaped Terpolymers. *J. Phys.: Condens. Matter* **2011**, *23*, 284111.
(24) Dotera, T. Toward the Discovery of New Soft Quasicrystals: From a Numerical Study Viewpoint. *J. Polym. Sci., Part B: Polym. Phys.* **2012**, *50*, 155−167.
(25) Zhang, J. W.; Bates, F. S. Dodecagonal Quasicrystalline Morphology in a Poly(styrene-b-isoprene-b-styrene-b-ethylene oxide) Tetrablock Terpolymer. *J. Am. Chem. Soc.* **2012**, *134*, 7636−7639.
(26) Lee, S.; Leighton, C.; Bates, F. S. Sphericity and Symmetry Breaking in the Formation of Frank-Kasper Phases from One Component Materials. *Proc. Natl. Acad. Sci. U. S. A.* **2014**, *111*, 17723−17731.
(27) Gillard, T. M.; Lee, S.; Bates, F. S. Dodecagonal Quasicrystalline Order in a Diblock Copolymer Melt. *Proc. Natl. Acad. Sci. U. S. A.* **2016**, *113*, 5167−5172.
(28) Chanpuriya, S.; Kim, K.; Zhang, J. W.; Lee, S.; Arora, A.; Dorfman, K. D.; Delaney, K. T.; Fredrickson, G. H.; Bates, F. S. Cornucopia of Nanoscale Ordered Phases in Sphere-Forming Tetrablock Terpolymers. *ACS Nano* **2016**, *10*, 4961−4972.
(29) Kim, K.; Schulze, M. W.; Arora, A.; Lewis, R. M., III; Hillmyer, M. A.; Dorfman, K. D.; Bates, F. S. Thermal Processing of Diblock Copolymer Melts Mimics Metallurgy. *Science* **2017**, *356*, 520−523.
(30) Bates, F. S.; Fredrickson, G. H. Block Copolymers - Designer Soft Materials. *Phys. Today* **1999**, *52*, 32−38.
(31) Grason, G. M.; DiDonna, B. A.; Kamien, R. D. Geometric Theory of Diblock Copolymer Phases. *Phys. Rev. Lett.* **2003**, *91*, 058304.
(32) Park, C.; Yoon, J.; Thomas, E. L. Enabling Nanotechnology with Self-Assembled Block Copolymer Patterns. *Polymer* **2003**, *44*, 6725−6760.
(33) Wickham, R. A.; Shi, A. C.; Wang, Z. G. Nucleation of Stable Cylinders from A Metastable Lamellar Phase in A Diblock Copolymer Melt. *J. Chem. Phys.* **2003**, *118*, 10293−10305.
(34) Li, W. H.; Wickham, R. A. Self-Assembled Morphologies of a Diblock Copolymer Melt Confined in a Cylindrical Nanopore. *Macromolecules* **2006**, *39*, 8492−8498.
(35) Hamley, I. W. Ordering in Thin Films of Block Copolymers: Fundamentals to Potential Applications. *Prog. Polym. Sci.* **2009**, *34*, 1161−1210.
(36) Qin, J.; Bates, F. S.; Morse, D. C. Phase Behavior of Nonfrustrated ABC Triblock Copolymers: Weak and Intermediate Segregation. *Macromolecules* **2010**, *43*, 5128−5136.
(37) Pang, X. C.; Zhao, L.; Han, W.; Xin, X. K.; Lin, Z. Q. A General and Robust Strategy for the Synthesis of Nearly Monodisperse Colloidal Nanocrystals. *Nat. Nanotechnol.* **2013**, *8*, 426−431.
(38) Li, W. H.; Nealey, P. F.; de Pablo, J. J.; Müller, M. Defect Removal in the Course of Directed Self-Assembly is Facilitated in the Vicinity of the Order-Disorder Transition. *Phys. Rev. Lett.* **2014**, *113*, 168301.
(39) Pang, X. C.; He, Y. J.; Jung, J.; Lin, Z. Q. 1D Nanocrystals with Precisely Controlled Dimensions, Compositions, and Architectures. *Science* **2016**, *353*, 1268−1272.
(40) Li, W. H.; Müller, M. Directed Self-Assembly of Block Copolymers by Chemical or Topographical Guiding Patterns: Optimizing Molecular Architecture, Thin-Film Properties, and Kinetics. *Prog. Polym. Sci.* **2016**, *54*−*55*, 47−75.
(41) Li, W. H.; Duan, C.; Shi, A. C. Nonclassical Spherical Packing Phases Self-Assembled from AB-Type Block Copolymers. *ACS Macro Lett.* **2017**, *6*, 1257−1262.
(42) Sun, D. W.; Müller, M. Process-Accessible States of Block Copolymers. *Phys. Rev. Lett.* **2017**, *118*, 067801.
(43) Leibler, L. Theory of Microphase Separation in Block Copolymers. *Macromolecules* **1980**, *13*, 1602−1617.
(44) Dotera, T.; Steinhardt, P. J. Ising-like Transition and Phason Unlocking in Icosahedral Quasicrystals. *Phys. Rev. Lett.* **1994**, *72*, 1670.
(45) Stampfli, P. A Dodecagonal Quasiperiodic Lattice in Two Dimensions. *Helv. Phys. Acta* **1986**, *59*, 1260−1263.
(46) Leung, P. W.; Henley, C. L.; Chester, G. V. Dodecagonal Order in a Two-Dimensional Lennard-Jones System. *Phys. Rev. B: Condens. Matter Mater. Phys.* **1989**, *39*, 446−458.
(47) Oxborrow, M.; Henley, C. L. Random Square-Triangle Tilings: A Model for Twelvefold-Symmetric Quasicrystals. *Phys. Rev. B: Condens. Matter Mater. Phys.* **1993**, *48*, 6966−6998.
(48) Matsen, M. W. The Standard Gausian Model for Block Copolymer Melts. *J. Phys.: Condens. Matter* **2002**, *14*, R21−R47.
(49) Fredrickson, G. H. *The Equilibrium Theory of Inhomogeneous Polymers*; Oxford, 2006.
(50) Arora, A.; Qin, J.; Morse, D. C.; Delaney, K. T.; Fredrickson, G. H.; Bates, F. S.; Dorfman, K. D. Broadly Accessible Self-Consistent Field Theory for Block Polymer Materials Discovery. *Macromolecules* **2016**, *49*, 4675−4690.
(51) Jiang, K.; Zhang, P. W. Numerical Methods for Quasicrystals. *J. Comput. Phys.* **2014**, *256*, 428−440.

DOI: 10.1021/acs.macromol.8b01638
Macromolecules 2018, 51, 7713−7721

(52) Xie, N.; Liu, M. J.; Deng, H. L.; Li, W. H.; Qiu, F.; Shi, A. C. Macromolecular Metallurgy of Binary Mesocrystals via Designed Multiblock Terpolymers. *J. Am. Chem. Soc.* **2014**, *136*, 2974−2977.
(53) Shi, A. C. *Development in Block Copolymer Science and Technology*; Wiley: New York, 2004.
(54) Tzeremes, G.; Rasmussen, K.; Lookman, T.; Saxena, A. Efficient Computation of the Structural Phase Behavior of Block Copolymers. *Phys. Rev. E: Stat. Phys., Plasmas, Fluids, Relat. Interdiscip. Top.* **2002**, *65*, 041806.
(55) Thompson, R. B.; Rasmussen, K. Ø.; Lookman, T. Improved Convergence in Block Copolymer Self-Consistent Field Theory by Anderson mixing. *J. Chem. Phys.* **2004**, *120*, 31−34.
(56) Ishimasa, T. Dodecagonal Quasicrystals Still in Progress. *Isr. J. Chem.* **2011**, *51*, 1216−1225.
(57) Matsen, M. W.; Bates, F. S. Origins of Complex Self-Assembly in Block Copolymers. *Macromolecules* **1996**, *29*, 7641−7644.
(58) Gao, Y.; Deng, H. L.; Li, W. H.; Qiu, F.; Shi, A. C. Formation of Nonclassical Ordered Phases of AB-Type Multiarm Block Copolymers. *Phys. Rev. Lett.* **2016**, *116*, 068304.
(59) Lei, T.; Henley, C. L. Equilibrium Faceting Shape of Quasicrystals at Low Temperatures: Cluster Model. *Philos. Mag. B* **1991**, *63*, 677−685.

DOI: 10.1021/acs.macromol.8b01638
Macromolecules 2018, 51, 7713−7721